Preinvasive Duct-Derived Neoplasms in Pancreas of Keratin 5−Promoter Cyclooxygenase-2 Transgenic Mice

KARIN MÜLLER–DECKER,* GERHARD FÜRSTENBERGER,* NADINE ANNAN,[†] DAGMAR KUCHER,* ANDREA POHL–ARNOLD,* BRIGITTE STEINBAUER,* IRENE ESPOSITO,[†] SARA CHIBLAK,* HELMUT FRIESS,[§] PETER SCHIRMACHER,[†] and IRINA BERGER[†]

*Eicosanoids and Tumor Development Section, Deutsches Krebsforschungszentrum, Heidelberg, Germany; and [†]Department of Pathology and [§]Clinic for Surgery, Department of General Surgery, Ruprecht-Karls-University, Heidelberg, Germany

Background & Aims: **Basic research aimed at a better understanding of pancreatic carcinogenesis and improving the treatment of this disease is crucial because the majority of pancreatic cancers are highly aggressive and therapeutically nonaccessible. Cyclooxygenase (COX)-2, which is a key enzyme of prostaglandin (PG) biosynthesis, is overexpressed in around 75% of human carcinomas including those of the pancreas.** *Methods:* **The pathologic changes of transgenic mouse pancreas with keratin 5−promoter-driven expression and activity of COX-2 were characterized.** *Results:* **Aberrant expression of COX-2 in a few ductal cells and COX-2−mediated PG synthesis in the transgenic mice resulted in keratin 19− and mucin-positive intraductal papillary mucinous neoplasm- and pancreatic intraepithelial neoplasia-like structures, characterized by an increased proliferation index and serous cystadenomas. Moreover, Ras activation was enhanced and the HER-2/Neu receptor was overexpressed. Loss of acini, fibrosis, and inflammation were pronounced. Feeding a COX-2−selective inhibitor to the transgenic mice suppressed the accumulation of PG and the phenotype. The changes resemble the human disease in which COX-2 was overexpressed consistently.** *Conclusions:* **We present strong evidence for a causal relationship between aberrant COX-2 overexpression and COX-2−mediated PG synthesis and the development of serous cystadenoma, intraductal papillary mucinous, and pancreatic intraepithelial neoplasms. This model offers the unique possibility of identifying molecular pathways leading to the formation and malignant progression of the various types of preinvasive lesions of pancreatic adenocarcinomas that show different dismal outcomes.**

Pancreatic ductal adenocarcinoma (PDAC) represents the major type of primary solid neoplasms of the exocrine pancreas. Cystic lesions of the exocrine pancreas are rare but increasingly recognized entities.[1,2] A new classification of the cystic pancreatic lesions was proposed[3] that provides a distinction based on biology (neoplastic/nonneoplastic) and clinical behavior (benign/borderline/malignant). According to these criteria and excluding the cystic variant of PDAC, intraductal papillary mucinous neoplasms (IPMNs), followed by serous cystic neoplasms, represent the most common cystic epithelial tumors of the exocrine pancreas. Serous cystic neoplasms, which almost always are benign, are lined by a flat to cuboidal, glycogen-rich epithelium that expresses cytokeratins 7, 8, 18, and 19 (ie, a profile that is typical of the ductal cells).[4] The immunohistologic profile and ultrastructural features suggest that serous cystic neoplasms originate from centroacinar cells of the pancreas.[5–7] At the genetic level, serous cystic neoplasms are distinguished clearly from other pancreatic cystic tumors.[8] IPMNs are defined as "grossly visible, noninvasive, mucin-producing, predominantly papillary, or rarely flat, epithelial neoplasms arising from the main pancreatic duct or branch ducts, with varying degrees of duct dilatation."[9] IPMNs can display a wide spectrum of cytologic and architectural atypia and therefore are classified further as benign (adenoma), borderline, and malignant (intraductal papillary mucinous carcinoma). Genetic studies have shown an accumulation of alterations in oncogenes (eg, K-ras, HER-2/Neu) and tumor-suppressor genes (eg, Ink4/Arf, Trp53) in the progression from IPMN adenoma to intraductal papillary mucinous carcinoma and invasive cancer[10–13] that only partially recapitulate the molecular alterations that characterize the progression from pancreatic intraepithelial neoplasia (PanIN) to invasive PDAC.[14] The microscopic papillary

or flat PanIN that arise from the small pancreatic ducts share common features with IPMNs, such as the intraductal neoplastic proliferations of columnar, mucin-containing cells with a variable degree of papillary growth. The columnar to cuboidal cells vary in the amount of mucin production and the degree of cytologic and architectural atypia.[9,15] Recently, transcriptomes of IPMN, PanIN, and PDAC were analyzed, showing the overexpression of distinct growth factors, cytokines, and proinflammatory proteins, including cyclooxygenase (COX)-2.[16–22]

Similar to COX-2, the second known active COX isoform in mouse and human beings, COX-1 converts arachidonic acid to prostaglandin (PG) H_2, which is metabolized by prostaglandin synthases into the bioactive PG.[23–25] A large body of evidence from epidemiologic,[26] genetic,[27–32] pharmacologic,[31,33,34] and clinical studies[35–37] show that COX-2 is involved causally in the neoplastic progression of epithelial cells in colon, breast, and skin. Moreover, COX-2 may play an important role in pancreatic tumorigenesis. In human beings a large portion of PanIN lesions[17] and the majority of PDACs,[17,38–41] serous cystadenomas (SCAs),[39] and IPMNs[18,42] were found to overexpress COX-2 as compared with normal duct epithelium of the pancreas. The constitutive expression of COX-1 was not modulated in the course of pancreatic tumor formation.[43,44] Moreover, selective COX-2[45] and nonselective COX inhibitors[46] repressed tumor growth in the hamster model of N-nitrosobis (2-oxopropyl)amine–induced pancreatic cancer and in an orthotopic pancreatic tumor xenograft model of the mouse.[47]

We previously reported on heterozygous keratin 5 promoter (K5) COX-2 transgenic mouse lines that developed a pancreatic phenotype.[29] The pancreatic phenotype of 4 heterozygous mouse lines ($675^{+/-}$, $667^{+/-}$, $663^{+/-}$, and $4^{+/-}$) and 1 homozygous mouse line ($675^{+/+}$) was diagnosed by pathologists and found to be similar, substantiating that the phenotype is transgene dependent and not caused by a positional effect. Here, we characterize in detail the pancreatic phenotype of the homozygous transgenic mouse line with keratin 5-driven COX-2 expression. We found a causal relationship between aberrant expression of COX-2 and COX-2–mediated PG synthesis in the pancreas and the development of dysplastic lesions characterized as SCA-like tumors and intraductal papillary mucinous lesions in large and small ducts that phenocopy human IPMN and PanIN. These changes were associated regularly with reactive changes in the surrounding parenchyma such as loss of acini and a fibroinflammatory reaction.

Materials and Methods

Materials

The following materials were used and purchased from sources as indicated. Enzyme-linked immunosorbent assay–bovine serum albumin (Sigma, Deisenhofen, Germany); polyclonal rabbit anti-mouse Ki67 (Novacastra, Neuss, Germany); alkaline phosphatase–conjugated anti-rabbit IgG, peroxidase-conjugated anti-rat IgG, Cy3-conjugated anti-rabbit IgG, and Cy3-conjugated anti-rat IgG (Dianova, Hamburg, Germany); goat polyclonal anti-β-actin (SC-1616), anti-human COX-2 (SC-1745), affinity-purified rabbit polyclonal anti-HER-2/ Neu-antibody (SC-284), and peroxidase-conjugated anti-rabbit IgG (SC-2020) and anti-mouse IgG (SC-2005) (Santa Cruz, Heidelberg, Germany); polyclonal rabbit anti-keratin 5 (Convance, Berkeley, CA); purified rat anti-mouse CD45R/B220 and CD4 (L3T4) monoclonal antibodies (BD Biosciences, Heidelberg, Germany); purified rat anti-mouse CD8α/Lyt-2 monoclonal antibodies (Southern Biotech, Birmingham, AL); rat anti-mouse F4/80 antiserum (Serotec, Düsseldorf, Germany); Alexa Fluor 488–conjugated anti-goat IgG (MobiTeC, Göttingen, Germany); PGE_2- and $PGF_{2\alpha}$-enzyme immunoassay kits (Cayman, Ann Arbor, MI); aprotinin, leupeptin, and α_2-macroglobulin (Roche Applied Sciences, Mannheim, Germany). Rat monoclonal anti-keratin 19 kindly was provided by R. Kemmler (Max-Planck-Institute, Freiburg, Germany).

Animals

K5 COX-2 transgenic lines $675^{+/+}$ and $667^{+/-}$ were generated and kept as described.[29,31] Age- and sex-matched wild-type (wt) Naval Medical Research Institute (NMRI) mice (outbred strain from RCC, Füllinsdorf, Switzerland) served as controls. Experiments were approved by the Governmental Committee for Animal Experimentation (license 053/00). Biopsy specimens were frozen immediately in liquid nitrogen or processed for histology or immunohistochemistry.

Treatments

To study the effect of a COX-2–selective inhibitor on the transgene-induced phenotype, a rodent diet 5010 (Purina Mills, St Louis, MO) containing 1500 ppm Celebrex (kindly provided by J. Masferrer, Pfizer, St Louis, MO) was fed to transgenic mice starting on day 1 after birth for 6–12 months. The diet was delivered to nursing mice for 4 weeks and later as regular chow.

Human Biopsy Specimens

Paraffin-embedded samples of normal pancreas (n = 5), IPMN borderline (n = 4), IPMN adenomas (n = 6), PanIN lesions (n = 10), SCAs (n = 5), and mucinous cystadenomas (n = 5) were selected from the archives of the Institute of Pathology at the University of Heidelberg and used for immunohistochemistry.

Immunoblot Analysis

Immunoprecipitation of COX isozymes and immunoblot analysis were performed as described using isozyme-specific antisera.[29,31] For immunodetection of Neu gp 185, frozen pancreas powder was homogenized in a HP buffer (50 mmol/L Tris/HCl, pH 7.4, 1% Tween 20, 2 mmol/L ethylenediaminetetraacetic acid, 1 mmol/L phenylmethylsulfonyl fluoride, 10 μg/mL aprotinin, 10 μg/mL leupeptin, and 2 mmol/L α_2-macroglobulin) and processed as described.[48] The specificity of the immunosignals was confirmed by complete quenching of the immunosignal on preadsorption of the antiserum with a 500-fold molar excess of the respective peptide antigen.

Ras Activation Assay

Ras activity was measured using a Ras Activation Assay Kit (Upstate, Lake Placid, NY) following the manufacturer's instructions. Briefly, frozen pancreas powder was homogenized in $1 \times Mg^{2+}$ lysis/wash buffer supplemented with 10 μg/mL each of aprotinin and leupeptin, 1 mmol/L sodium orthovanadate, and 25 mmol/L sodium fluoride, and kept on ice for 60 minutes. Lysates were centrifuged at $14,000g$ for 5 minutes. From the supernatant, 2 mg of protein each were used for a positive control (guanosine 5′-triphosphate [GTP]-γ-S–loaded at 30°C for 30 min), a negative control (guanosine 5′-diphosphate [GDP]-loaded at 30°C for 30 min), and a mock-treated sample. After termination of loading, Ras GTP was affinity precipitated from each sample using 20 μg of Ras assay reagent (Raf-1 Ras binding domain agarose/glutathione agarose beads) for 60 minutes at 4°C. The precipitates were washed 3 times with $1 \times Mg^{2+}$ lysis/wash buffer and denatured in 40 μL $1 \times$ Laemmli sample buffer and 1 mmol/L phenylmethylsulfonyl fluoride. Together with a recombinant p21 H-Ras[Gly-12] as positive control (Oncogene, Boston, MA), the proteins were separated on a 15% sodium dodecyl sulfate–polyacrylamide gel. Ras protein was immunodetected with purified mouse monoclonal anti-Ras IgG2ακ (clone RAS 10, diluted 1:20,000) in blocking reagent (5% milk powder in phosphate-buffered saline, 0.1% Tween 20). Proteins were visualized with a goat anti-mouse secondary antibody horseradish-peroxidase conjugate and enhanced chemiluminescence detection (GE Healthcare BioSciences, Freiburg, Germany). To normalize the amount of GTP-bound Ras to the total amount of Ras, 120 μg/lane of ethanol-precipitated lysate protein were co-analyzed by immunoblotting as described earlier. As additional loading controls, 60 μg of protein of each sample were separated by 7.5% sodium dodecyl sulfate–polyacrylamide gel electrophoresis and stained with Coomassie brilliant blue. A quantitation of protein density (integrated density value) in each lane was performed by means of the spot denso module of the AlphaEase software of the ChemiImager (Biozym, Hess, Oldendorf, Germany). As a positive control for activated Ras we used a skin papilloma gained from a 2-stage carcinogenesis experiment.[31]

Histochemistry and Immunohistochemistry

Cryosections of mouse pancreas (5 μm) were used for H&E staining. Paraffin-embedded tissue sections (5 μm) served for staining of acidic mucopolysaccharides with Alcian blue (Sigma, Deisenhofen, Germany) and collagen fibers with Masson Goldner according to a routine protocol. Immunohistochemical (CD4, CD8, CD45R/B220, and COX-2) and immunofluorescence analysis (COX-2, keratin 5, keratin 19, Ki67, and F4/80) of mouse tissue were performed with 5-μm cryosections fixed in acetone for 10 minutes and processed as published.[31] Primary antibodies were diluted 1:50–1000 and peroxidase- or fluorochrome-conjugated secondary antibodies 1:100–2000 in blocking solution. Ki67-positive cells were determined as the percentage of the total number of ductal cells counted, which were counterstained with Hoechst dye 33258. COX-2 immunostaining of human paraffin-embedded specimens was performed with COX-2 antibodies diluted 1:100 in phosphate-buffered saline with 1.5% normal horse serum and an incubation for 2 hours at room temperature.[48] Negative controls included sections incubated without primary or with the isotype-matched primary antibody.

Electron Microscopy

Two-millimeter tissue specimens were fixed in 3% glutaraldehyde and embedded in Epon. Semithin and ultrathin sections were prepared for microscopy according to a routine procedure. Electron microscopy was performed using a Zeiss analytical EM 902 (Oberkochen, Germany) coupled with a Pro-Scan digital camera (Troendle, Munich, Germany).

Determination of PG Levels

PGE_2 and $PGF_{2\alpha}$ contents (mean pg/mg protein $\pm$ SD, $n \geq 5$) were determined as described.[31]

Statistical Analysis

Student t tests were performed and P values less than .05 were regarded as significant.

Results

Gross Phenotype of the K5 COX-2 Transgenic Pancreas

Beginning at the age of 3 months transgenic mice of the homozygous line K5 COX-2/675[+/+] showed up with dramatically enlarged polycystic pancreata. The cystic structures were connected to the ductal systems. In initial stages the cysts contained serous clear watery fluid, whereas late-stage cysts tended to be hemorrhagic (Figure 1A). The incidence of polycystic pancreata increased with age and affected about 31% of the mice at 12 months of age. Such a phenotype was not observed in wt mice (Figure 1B).
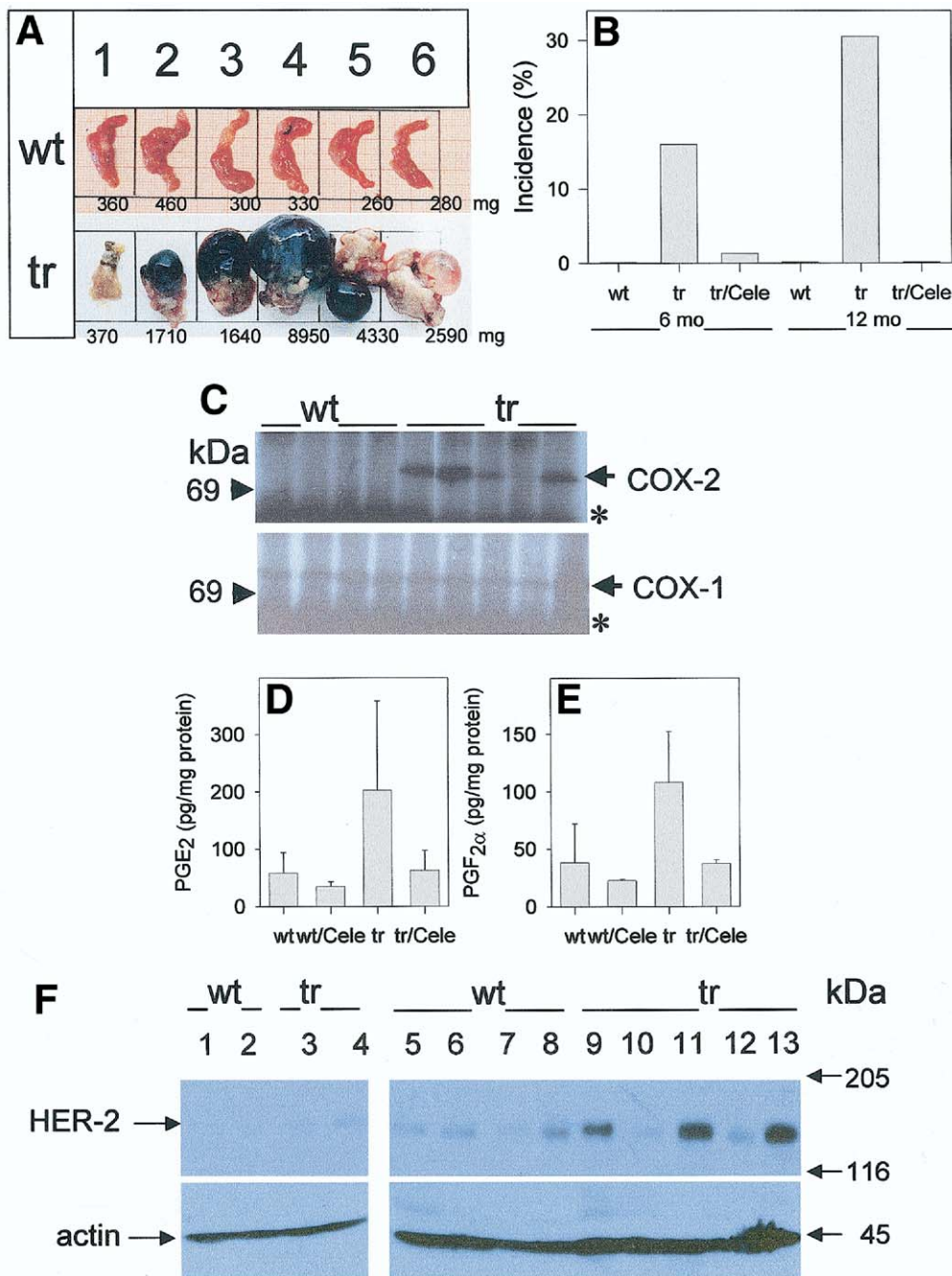
Figure 1. Keratin 5-promoter–driven overexpression of COX-2 and COX-2–mediated PG synthesis in pancreata of transgenic mice, gross phenotype, and HER-2 expression. (*A*) Gross phenotype and weight (mg) of normal wt and polycystically enlarged transgenic (tr) pancreata from 6 mice each. (*B*) Incidence of cystic pancreas in wt, tr, and tr fed with Celebrex (Cᴇʟᴇ) throughout 6 or 12 months of postnatal life. Cohorts of 20 wt mice/group and of 80 (6 mo) and 60 (12 mo) tr mice/group were followed up. (*C*) COX-2 and COX-1 protein levels in pancreas of wt (n = 4) and tr (n = 5) mice. COX isozymes were immunoprecipitated consecutively from pancreatic protein homogenates and detected by immunoblotting using COX isozyme–specific antisera. *IgG cross-reaction with the secondary antibody. (*D*) PGE_2 levels in pancreas of 6-month-old wt and tr mice fed control diet or diet containing Celebrex (Cᴇʟᴇ) for 6 months after birth. Differences in PGE_2 levels between wt (n = 8) and tr (n = 10), and tr (n = 10) and tr/Cele (n = 8) were statistically significant (Student *t* test: $P < .022$ and $< .025$, respectively), whereas all other test combinations were $P > .05$. (*E*) $PGF_{2\alpha}$ levels in pancreas of 6-month-old wt and tr mice fed control diet or diet containing Celebrex (Cᴇʟᴇ) for 6 months after birth. (*F*) Increased steady-state levels of HER-2/Neu receptor protein in the tr as compared with wt pancreas. Immunoblot analysis of extracts from pancreata of 7-week-old (*lanes 1 and 2*) and 10-month-old wt (*lanes 5–8*), 7-week-old (*lanes 3 and 4*) and 8–12-month-old (*lanes 9–13*) tr mice using anti-human HER-2/Neu receptor antibodies to detect HER-2/Neu and anti–β-actin antibodies to detect β-actin as loading control. Marker proteins are given in kilodaltons (kDa).

Overexpression and Activity of COX-2 in Transgenic Pancreas

Because the keratin 5 promoter is known to be active in a few epithelial cells of pancreatic ducts,[49,50] (see later) the transgenic phenotype was expected to correlate with aberrant COX-2 overexpression. In fact, COX-2 protein was detected in 8 of 8 homozygous K5 COX-2/$675^{+/+}$ transgenic pancreata, whereas COX-2 protein was less than the level of detection in wt pancreas (n = 6). COX-1 protein expression was similar in the pancreas of both groups (Figure 1C). The levels of PGE_2 and $PGF_{2\alpha}$ were increased in the pancreas of transgenic mice as compared with wt controls (Figure 1D and E). When K5 COX-2/$675^{+/+}$ mice were fed the COX-2–selective inhibitor Celebrex[51] for up to 6 or 12 months postnatally, pancreatic PGE_2 and $PGF_{2\alpha}$ contents were suppressed to near basal levels measured in wt pancreas (Figure 1D and E), which reflect the activity of the constitutively expressed COX-1. Under these conditions, the observed gross phenotype of polycystic pancreas did not develop (Figure 1B).

Histopathology of the K5 COX-2 Transgenic Pancreas

Although the monolayered ductal epithelium of pancreas of wt mice is surrounded by abundant acinar tissue with scattered Langerhans' islets and blood vessels (Figure 2A), extensive histologic alterations within the ductal, acinar, and stromal compartments were observed in the transgenic pancreas. Characteristic features were large cystically dilated ducts partially lined by a single layer of epithelial cells (Figure 2B and C). Furthermore, large dilated ducts with intraductal papillary hyperplasia were observed (Figure 2D). In addition, multiple small ducts with prominent lumen were present within the lobules (Figure 2E and F). These changes were associated frequently with a loss of acini (Figure 2E and F) and the presence of an inflammatory infiltrate throughout the pancreas (Figure 2F). A histopathologic analysis of pancreata from 3- (n = 10), 6- (n = 13), and 12-month-old transgenic mice (n = 18) showed that inflammatory changes did not occur before changes in the ducts. In large areas of the pancreas, a periductal fibrosis was distinct (Figure 2G) and the acinar parenchyme was replaced by fibrotic tissue (Figure 2H), as indicated by the positive histochemical Masson Goldner stain.

Inflammatory Infiltrate in the K5 COX-2 Transgenic Pancreas

The cell types of the inflammatory infiltrate in transgenic pancreas were phenotyped by immunostaining using spleen as positive control (data not shown) as F4/80-positive macrophages, CD45R/B220-positive B lymphocytes, and CD4 (L3T4)-positive T lymphocytes. CD8α/Lyt-2–positive T lymphocytes rarely were present (Figure 3). Lymphocytes were localized throughout the pancreas (eg, adjacent to the ducts and in the vicinity of the residual acinar epithelium and Langerhans' islets). No inflammatory cells were detectable in wt pancreatic tissue (Figure 3).

Ductal Dysplasia in the K5 COX-2 Transgenic Pancreas

When compared with the single layer of flat to cuboidal epithelial duct cells with uniform round nuclei in the intralobular and interlobular ducts of wt controls (Figure 4A and B), the observed lesions displayed different degrees of dysplasia. In some cases they were lined by columnar cells with basally located nuclei and supranuclear enlarged cytoplasm (Figure 4C), or they displayed papillary hyperplasia with minor loss of nuclear polarity (Figure 4D and E). In other cases, the cells of the hyperplastic epithelium were characterized by a loss of nuclear polarity and by a weak to moderate nuclear enlargement and hyperchromasia (Figure 4F). These cytologic atypias were seen in larger cystic ducts (Figures 4C–F and 5C) and in small intralobular ducts (Figures 4G–I and 5I, M, and O), and overall they resembled human IPMNs and PanINs, respectively. These intraductal hyperplastic lesions were accompanied in one third of cases by tubular structures with high-grade cell atypia and high mitotic activity (Figure 4J and K), but lacking clear signs of invasion. Another type of cystic lesions characterized by a single layer of uniform low cuboidal to flat cells lacking atypical nuclei was observed (Figure 4L and M) that phenocopy human SCA.

Molecular Markers of Ductal Lesions in the K5 COX-2 Transgenic Pancreas

Wt pancreas expressed COX-2 neither in ductal nor in islet cells, but only in blood vessel cells (Figure 5A). In contrast, blood vessel and epithelial duct cells within nonlesional (Figure 5B) and dysplastic papillary lesions of transgenic pancreas were COX-2 positive (Figure 5C and D), in part colocalizing with keratin 5 in large (Figure 5E–G) and small ducts (data not shown). The IPMN-like and the PanIN-like structures expressed the duct-specific marker keratin 19 throughout these structures (Figure 5H and I). In part, COX-2 colocalized with keratin 19, indicating the up-regulation of endogenous COX-2 expression (shown for small ducts Figure 5I–K). Moreover, cells within the lesions were Alcian blue–positive in the apical cytoplasm (Figure 5L and M), which is consistent with the presence of mucin that is
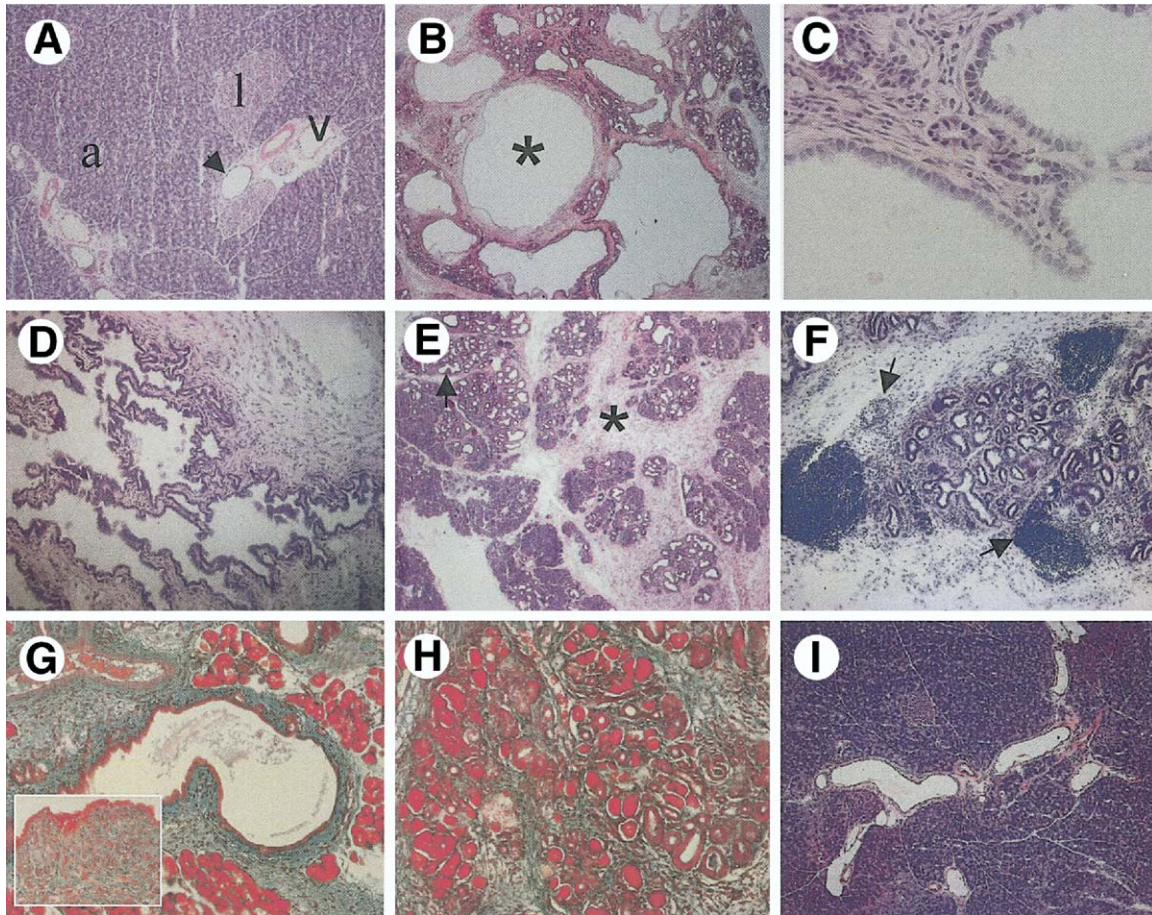
Figure 2. Abnormal ducts, loss of acini, proinflammatory infiltrate, and fibrosis in the K5 COX-2 transgenic pancreas. (*A*) Pancreas of a wt mouse with abundant acinar parenchyme (a) surrounding ductal epithelium (arrow), islets (l), and blood vessels (v). (*B–I*) Pancreas of tr mice. (*B*) Cystically dilated ducts shown by asterisk. (*C*) Cystically dilated ducts built up by a monolayer of epithelium. (*D*) Large cystically dilated duct with intraductal papillary hyperplasia resembling human IPMN. (*E*) Loss of acinar parenchyma shown by asterisk and ductal proliferation of tubular structures, which in part showed up with intraductal papillary hyperplasia (arrow). (*F*) Inflammatory infiltrates (arrows). (*G*) Masson Goldner–positive green staining indicating a fibrotic reaction in periductular pancreas. (*H*) Masson Goldner–positive green staining of tissue indicating a fibrotic reaction in intralobular pancreas. (*I*) Suppression of the pathologic phenotype in the pancreas of a 12-month-old tr mouse fed with Celebrex diet throughout life. Magnifications are as follows: (*A*) 1.25×, (*B*) 2.5×, (*D–F, I*) 10×, (*G, H*) 16×, and (*C*) 40×.

produced by duct cells of normal pancreas.[52] Furthermore, IPMN- and PanIN-like lesions of transgenic pancreas showed a significantly increased Ki67 labeling index (33.3% ± 4% SEM positive of 4353 duct cells, n = 3 mice), as compared with wt controls (6.0% ± 1% SEM positive of 2034 cells, n = 3 mice (Figure 5*N* and *O*), Student t test: $P < .00005$), emphasizing the hyperproliferative character of these lesions.

In contrast, the COX-2– and keratin 19–positive cells (Figure 5*P* and *Q*) of SCA-like ductal structures (Figure 4*L* and *M*) did not produce mucin (data not shown) but contained glycogen within their cytoplasm (Figure 5*R*), which is characteristic for SCA of human beings.[5] According to immunolabeling with Ki67, the proliferation index of SCA-like lesions (12.5% ± 4.5% SEM Ki67-positive of 990 cells, n = 3) was not significantly different from that of wt ducts (Student t test: $P = .204$),

but significantly lower than in IPMN- and PanIN-like lesions (Student t test: $P < .005$).

Celebrex Suppresses the Pancreatic Dysplasia of the K5 COX-2 Transgenics

Transgenic mice fed Celebrex (Figure 1*B*, *D*, and *E*) developed neither SCA-, IPMN-, nor PanIN-like structures nor a loss of acinar epithelium, inflammation, or fibrosis (Figure 2*I*). In line with this observation, the Ki67 proliferation index (3.3% ± 1% SEM positive of 3127 cells, n = 3 mice) was significantly different from the index determined for the transgenic mice that were fed the control diet (Student t test, $P < .00005$). In fact, pancreatic morphology resembled that of wt tissue (Figure 2*A*). The results show that the development of the transgenic phenotype was related causally to the COX-2–mediated PG synthesis.
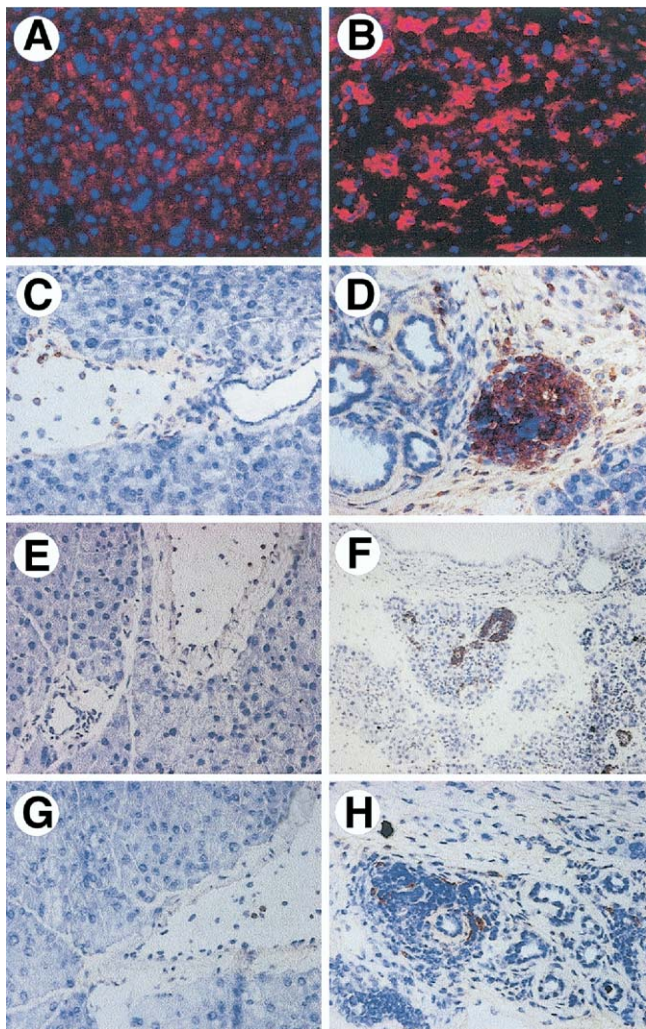
Figure 3. Phenotyping of the inflammatory infiltrate in the K5 COX-2 transgenic pancreas. Detection of (*A*, *B*) F4/80, (*C*, *D*) CD45, (*E*, *F*) CD4, and (*G*, *H*) CD8 in (*A*, *C*, *E*, *G*) wt and (*B*, *D*, *F*, *H*) transgenic pancreas by (*A*, *B*) indirect immunofluorescence or (*C*–*H*) immunohistochemistry. In wt pancreas (*A*) no macrophages were observed, whereas (*C*) CD45-, (*E*) CD4-, and (*G*) CD8-positive lymphocytes were detected within blood vessels, but not in the exocrine or endocrine pancreas. Note the presence of (*B*) F4/80-positive macrophages, (*D*) CD45-positive B cells, and (*F*) CD4-positive T cells in the transgenic pancreas. (*H*) CD8-positive T cells were rare. Magnifications are as follows: (*F*) 16×, and (*A*–*E*, *G*, *H*) 40×.

HER-2/Neu Expression Levels in the K5 COX-2 Transgenic Pancreas

A characteristic molecular change that occurs early during pancreatic ductal adenocarcinogenesis in human beings is the overexpression of HER-2/Neu in PanIN and IPMN lesions.[15,53] An immunoblot analysis of the HER-2/Neu receptor status in the pancreas of 7-week-old wt and transgenic, 10-month-old wt, and 8−12-month-old K5 COX-2 transgenic animals showed an increased level of HER-2/Neu receptor protein in the transgenic tissue (Figure 1*F*). There seems to be a cor-

relation between the macroscopically visible phenotype (ie, the size of the cyst) and the expression level of HER-2.

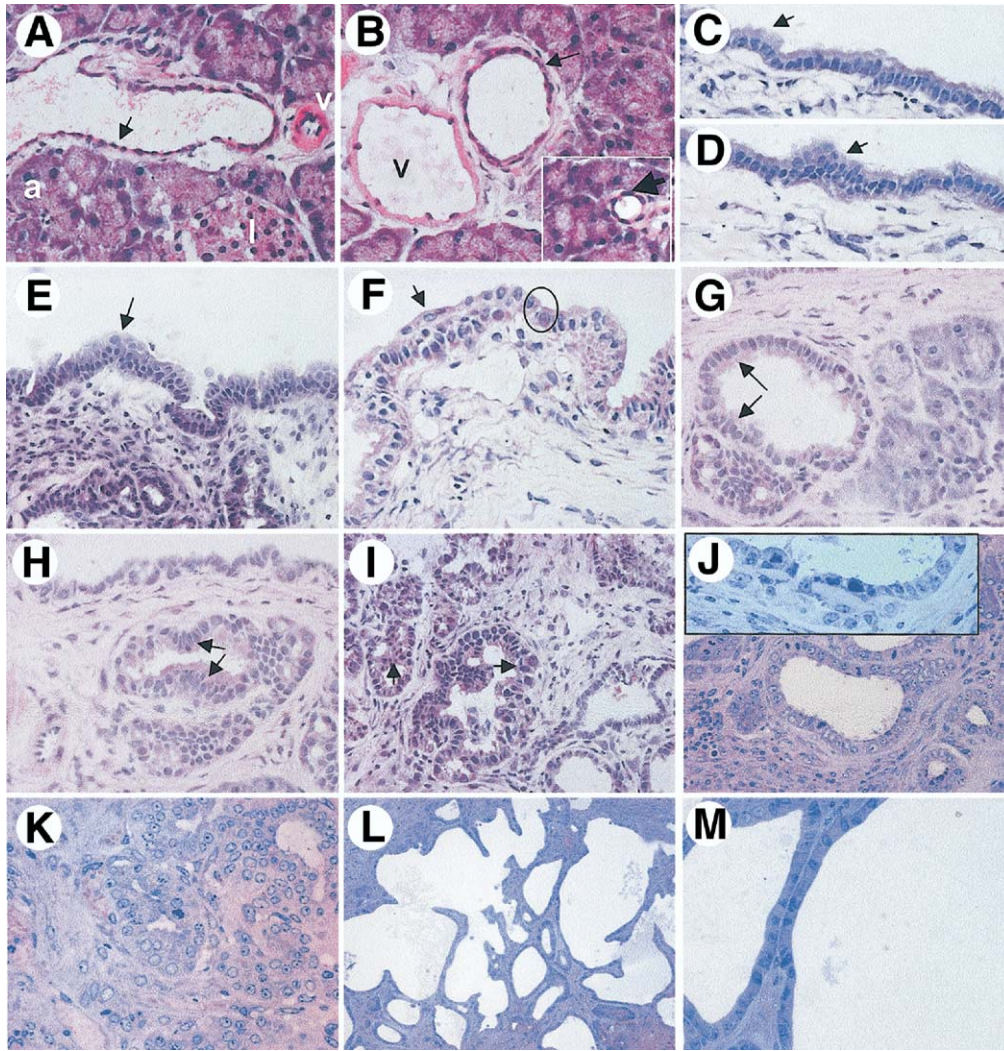### Ras Activation in K5 COX-2 Transgenic Pancreas

Because ras activation is known to represent an early change in pancreatic carcinogenesis,[15] a Ras activation assay was performed by selective affinity precipitation of GTP-bound Ras with Raf-1 Ras binding domain−conjugated agarose and subsequent immunoblot detection of Ras with a pan-Ras antibody (Figure 6). As compared with wt and nonlesional transgenic pancreas, the steady-state levels of Ras protein were increased about 3.5-fold in lesional transgenic pancreas (Figure 6*A*). When normalized to total Ras, the Ras−GTP levels were increased in transgenic lesional pancreas as compared with both nonlesional transgenic and wt pancreas by about 1.8-fold (Figure 6*B* and *D*). Increased Ras−GTP levels also were found in lysates of mouse papillomas known to carry a mutated Ras and therefore represent an appropriate positive control (Figure 6*C*).[31] In an independent experiment, Celebrex treatment of transgenic mice was shown to suppress both the transgene-induced expression and Ras activity (Figure 6*A* and *B*).

COX-2 Overexpression in Dysplastic and Neoplastic Human Pancreas

Given that the pancreas of transgenic mice showed signs of both PanIN-like, IPMN-like, and serous cystic neoplasm−like structures, COX-2 expression was examined within these human dysplasias and neoplasias. All the IPMN borderline, IPMN adenoma, PanIN lesions, SCA, and mucinous cystadenomas investigated showed a moderate to strong cytoplasmic COX-2 immunoreactivity in the duct epithelium (shown representatively in Figure 7*A*–*H*). In addition, slight focal COX-2 immunoreactivity was found in the cytoplasm of islet cells, although the mesenchyme, endothelium, and acinar epithelium were COX-2 negative. In normal human pancreatic tissue only weak COX-2 immunosignals were detected in few duct cells and cells of islets of Langerhans. Acinar epithelium was negative for COX-2 (see Figure 7*I* for a representative picture).

Discussion

As previously reported, keratin 5-promoter−driven COX-2 overexpression and activity in basal epithelial cells spontaneously caused hyperplasia and dysplasia in the skin[29] and the urinary bladder[54] in a COX-2− and PG-dependent manner. Moreover, transi-

Figure 4. SCA-, IPMN-, and PanIN-like structures in K5 COX-2 transgenic pancreas. (*A*) Wt pancreas with normal interlobular duct epithelium built up by a single layer of cuboidal cells (longitudinal section, arrow). v, blood vessel; I, Langerhans' islet; a, acinar parenchyme. (*B*) Cross-sectioned interlobular and intralobular (inset) duct epithelium (arrows) in pancreas of wt mice. v, blood vessel. (*C–M*) In transgenic pancreas the following changes were observed. (*C*) Columnar epithelium with basally located nuclei and supranuclear enlarged cytoplasm (arrow) in interlobular duct; (*D*) micropapillary hyperplasia (arrow) in interlobular duct; (*E*) papillary hyperplasia in interlobular duct with a weak loss of cell polarity (arrow); (*F*) IPMN-like lesion resembling human IPMN borderline lesions. Note the papillary hyperplasia in interlobular duct with loss of cell polarity (arrow) and nuclear atypia including hyperchromatism (encircled). (*G*) PanIN-like structure of low-grade dysplasia (similar to human PanIN 1A/1B) in intralobular duct (arrows). Note the columnar cells with the basally located nuclei and the supranuclear mucin. (*H*) PanIN-like structures in intralobular duct (arrows) resembling human PanIN 2. Note the mucinous epithelium with papillary architecture and the nuclear crowding and some enlarged nuclei. (*I*) PanIN-like structures in intralobular ducts (arrows) resembling human PanIN 3. Note the papillary structure of the epithelium and the budding off of cells into the lumen and the increased number of atypic nuclei. Invasion of the basement membrane is not observed. (*J*, *K*) Tubular structures with high-grade cell atypia and atypical mitotic figures (*J*, inset). (*L*, *M*) SCA-like structures showing the flat monolayer of cuboidal epithelium. Cell atypias were not observed. (*A–I*) H&E-stained 5-μm cryosections, (*J–M*) semithin sections stained with methylene blue. Magnifications are as follows: (*A–D*, *F*, *G*, *H*, *K*, *J*, inset, *M*) 63×, (*E*, *I*, *J*) 40×, and (*L*) 16×.

tional cell carcinomas were induced spontaneously in the urinary bladder,[54] whereas mouse skin was sensitized for carcinogenesis.[31] Hyperproliferative and dysplastic lesions also were induced in other keratin 5-positive epithelia such as the mammary gland[48] and, as shown here, the pancreas. Targeting COX-2 to distinct ductal cells of the pancreas by the keratin 5 promoter caused strong overexpression of COX-2 and highly increased PGE_2 and $PGF_{2\alpha}$ levels and resulted in dysplastic lesions. Suppres-

sion of PG synthesis by the COX-2–selective inhibitor Celebrex prevented both the accumulation of PG and the transgenic phenotype supporting a cause-and-effect relationship between aberrant COX-2 expression/activity and the development of dysplastic lesions. According to histologic analysis they represent a mixed pattern of lesions that resemble human SCA, IPMN, and PanIN. Interestingly, these benign human neoplasias are shown to overexpress COX-2 as compared with the normal duct epithelium,

confirming published data.[17,18,39,42] In human beings, these dysplastic lesions are assumed to arise from centroacinar cells and cells of large and small ducts, respectively.[7,9]


The initial target of the keratin 5-promoter–driven expression of the transgene are keratin 5-positive cells, which represent a minor fraction of about 5% of ductal cells.[49,50,52] In fact, this keratin 5-positive subpopulation, which, according to preliminary data, also was keratin 19 positive, constitutively expressed COX-2. Yet COX-2 also was expressed in keratin 5-negative/keratin 19–positive duct cells. This points to an up-regulation of endogenous COX-2 in this cell type, whereas other keratin 5-negative cells, including acinar or islet cells, did not express COX-2. This supports the view that aberrant expression of COX-2 in ductal epithelium is responsible for the development of the transgenic phenotype.

SCA-like lesions also were observed in Ink4a/Arf- and Trp53-deficient mice when crossed with metallothionein–transforming growth factor α transgenic mice,[55] although mutations in the Ink4a/Arf and Trp53 genes were not found in human SCA.[8] In our model, the development of cystic IPMN-like lesions graded as borderline was more prominent than the occasionally occurring intraductal hyperplasia found in transgenic mice with keratin 19 promoter–driven overexpression of the mutant K-rasG12V oncogene.[56]

The PanIN-like lesions staged 1B–3 that occurred in small ducts of COX-2 transgenic pancreas were at least in part qualitatively similar to the PanINs observed in transgenic mice that carried the mutated K-rasG12D
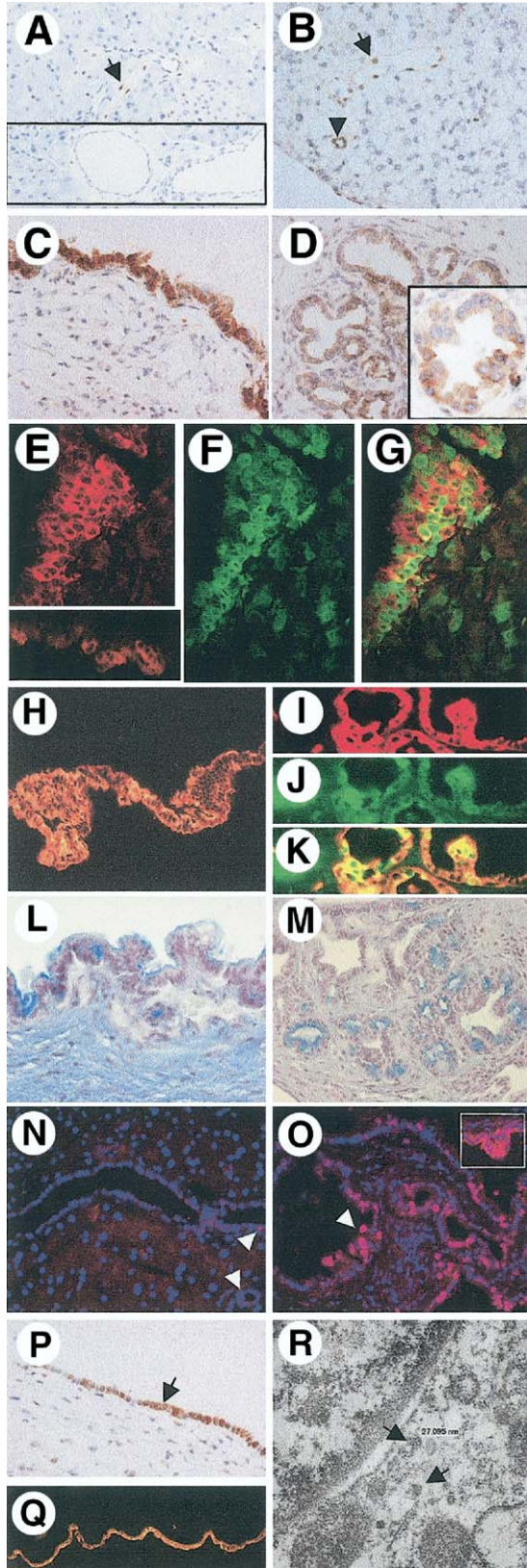
Figure 5. Characterization of SCA-, IPMN-, and PanIN-like structures in the K5 COX-2 transgenic pancreas. (*A–D, P*) Immunohistochemical or (*E–K, N, O, Q*) immunofluorescence analyses are presented. (*A*) COX-2 protein in blood vessels (arrow) but not in ducts (inset), acinar parenchyme, or islets of wt pancreas. (*B*) COX-2 protein in blood vessels (arrow) and in small ducts (△) of nonlesional pancreas of transgenic mice. (*C*) COX-2 protein in the epithelium of an IPMN-like lesion. (*D*) COX-2 protein in intralobular tubular duct-like structures and PanIN-like lesions (inset). (*E–G*) Double immunofluorescence analysis using anti-keratin 5 and anti–COX-2 antisera showed (*E*, red signals) keratin 5 and (*F*, green signals) COX-2 colocalization in the (*G*, yellow/orange signals) hyperplastic ducts. (*E*, inset) Focal keratin 5 expression in ducts of the transgenic pancreas. (*H*) Expression of ductal cell marker keratin 19 in an IPMN-like lesion. (*I–K*) Double immunofluorescence analysis using anti–keratin 19 and anti–COX-2 antisera showed that (*I*, red signals) keratin 19 and (*J*, green signals) COX-2 colocalize in (*K*, yellow/orange signals) PanIN-like structures. (*L, M*) Alcian blue stain shows mucin content in (*L*) IPMN-like and (*M*) PanIN-like lesions. (*N, O*) The level of expression of Ki67 (red) in ducts (arrows) was low in the pancreas from (*N*) wt mice and was increased in (*O*) large and small ducts of the transgenic pancreas. Note the (*O*, arrow) hyperproliferative PanIN-like and (*O*, inset) IPMN-like lesion. Nuclei are counterstained in blue with Hoechst dye 33258. (*P*) COX-2 protein in the single-layered SCA epithelium (arrow). (*Q*) Keratin 19 protein throughout the single-layered SCA epithelium. (*R*) Cytoplasmic glycogen deposits (arrows) in a cell of an SCA-like lesion as shown by electron microscopy. Magnifications are as follows: (*A–D, H, M–P,* and *A* inset) 40×, (*E–G, I–L,* and *D, E,* and *O* insets) 63×, (*Q*) 16×, and (*R*) 31,200×.
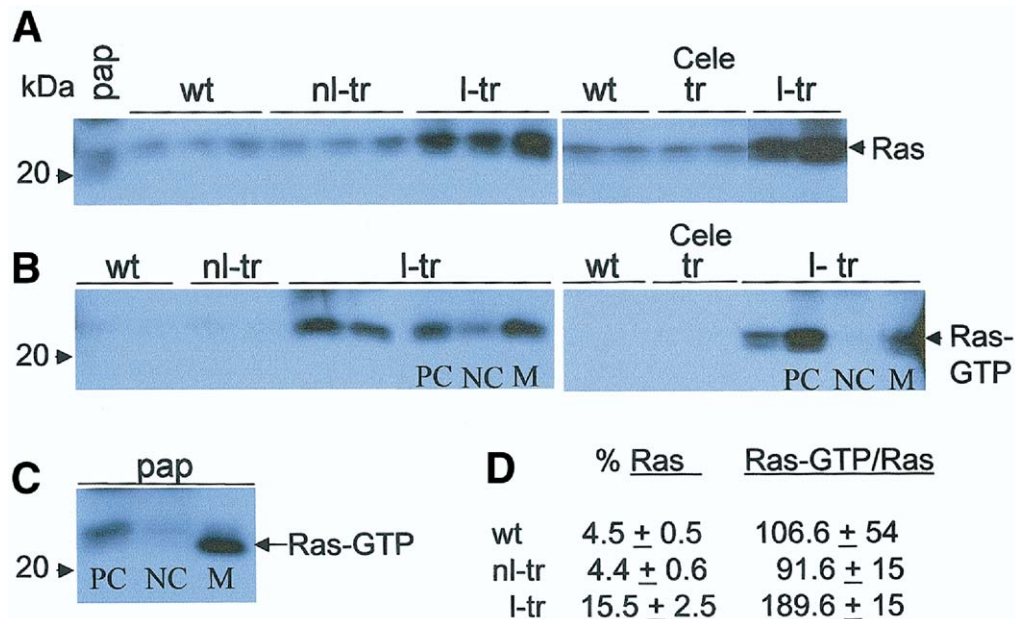
Figure 6. Increased Ras and Ras-GTP levels in lesional pancreas of K5 COX-2 transgenic mice. Representative signals from 2 independent experiments evaluating (*A*) total Ras and (*B, C*) Ras-GTP levels in 2 mg of protein lysate from age-matched wt (n = 6), nonlesional transgenic (nl-tr, n = 3) and lesional transgenic (l-tr, n = 6) pancreas exposed to control diet, transgenic pancreas exposed to Celebrex for 12 months (CELE tr, n = 3), and from skin papilloma (pap) (n = 2) including positive controls (PC), that is, lesional transgenic pancreas loaded in vitro with GTP-γ-S; negative controls (NC), that is, lesional pancreas loaded in vitro with GDP and mock-treated (M) lysates. Affinity precipitation of Ras-GTP was performed with the Ras assay reagent. Ras and Ras-GTP were probed with a monoclonal anti-Ras antibody. (*D*) Semiquantitative evaluation of the signal intensities was performed by the AlphaEase software and expressed as integrated density values (IDV). Mean values ± SEM of 3 samples of experiment 1 are given for relative (%) Ras levels (IDV Ras/IDV total protein) and relative Ras-GTP levels (IDV Ras-GTP/IDV total Ras) of wt, nonlesional transgenic, and lesional transgenic pancreata. Mean IDV ± SEM (n = 3) for total protein lysates of pancreata for wt were: $1.46 \times 10^5 \pm 3552$; for nonlesional transgenic were: $1.50 \times 10^5 \pm 2926$; and for lesional transgenic pancreata samples were: $1.38 \times 10^5 \pm 7105$. In *A* and *B*, the left panels are representative for experiment 1 and the right panels are representative for experiment 2.

under the control of the pancreatic duodenal homeobox (PDX)-1 or the PTF-1–p48 promoter, which both are active in undifferentiated PDX-1–, PDX-1/PTF-1–p48–positive pancreatic precursor cells during development or in the adult organ in PDX-1–positive mature endocrine or PTF-1–p48–positive mature acinar cells.[57,58] Acinar or islet tumors were not observed.[57] In line with this result, the targeting of mutated K-ras to adult acinar or ductal cells did not cause the formation of PanIN lesions.[56,59] Pancreata of transgenic mice with PDX-1–promoter–driven misexpression of sonic hedgehog in the pancreatic endoderm also developed dysplastic lesions with K-ras mutations resembling early stage PanINs in human beings.[60] Because keratin 5-positive cells were the target population of our COX-2 construct the position of keratin 5-positive ductal cells within the pancreatic differentiation program[61,62] remains to be defined, in particular whether or not this ductal cell type represents a descendant of an undifferentiated pancreatic PDX-1–positive/keratin 19–negative precursor cell or is a precursor of terminally differentiated PDX-1–negative/keratin 5-negative/keratin 19–positive cells.

IPMN are known to grow predominantly in the main pancreatic duct, the secondary ducts, or both, and also may involve the branch ducts or even extend into the smallest caliber pancreatic ducts, thereby mimicking PanINs.[9] The reverse has been described for PanIN involving the main pancreatic duct.[63] Because COX-2 was targeted to keratin 5-positive cells of both small and large ducts, the coexistence of IPMN- and PanIN-like lesions in COX-2 transgenic mice may suggest that the 2 types of lesions may have developed independently.

Consistent with the nature of human IPMNs and PanINs,[9,15] the corresponding counterparts in COX-2 transgenic pancreas expressed the epithelial cell marker keratin 19, contained mucin, and were hyperproliferative. A histopathologic analysis of pancreata from 3- to 12-month-old transgenic mice showed that the inflammatory changes did not occur before duct proliferation, suggesting that epithelial proliferation may not be caused by a reactive effect induced by the inflammatory cells.

The stimulation of growth correlated with increased PGE_2 and $PGF_{2\alpha}$ levels. This observation is in line with
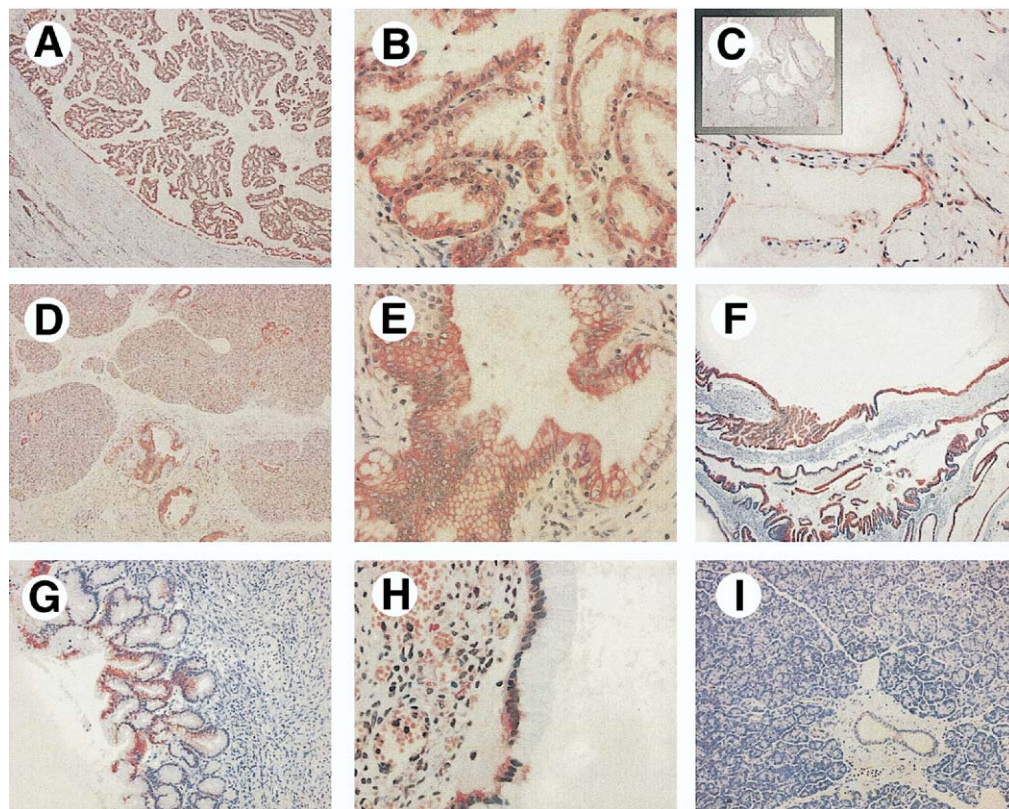
Figure 7. COX-2 expression in dysplastic and neoplastic human pancreatic tissue. Representative pictures of the cytoplasmic COX-2 immunostainings. Diffuse moderate signals in the tumor cells of an (*A, B*) IPMN borderline and a (*C*) serous microcystic adenoma. (*D, E*) PanIN 1A and 1B with weak to moderate signals. (*F, G*) Diffuse weak to moderate signals in epithelial cells of a mucinous cystic neoplasm with ovarian-like stroma. (*H*) Weak diffuse signals in epithelial cells of a mucinous cystadenoma. (*I*) Weak signals in interlobular ducts of normal pancreas. Magnifications are as follows: (*A, C* inset, *D, F*) 3×, (*I*) 7.8×, (*C, G*) 15.6×, (*B, H*) 31.2×, and (*E*) 42×.

a previous study that showed a growth-stimulatory effect of PG synthesis on pancreatic cancer cells in vitro.[16,38] A growth-stimulatory activity of PGE_2 is not unique to pancreatic cancer cells, but also was reported for colon cancer cells and seems to be caused by a transactivation of epidermal growth factor receptor[64] or the induction of amphiregulin.[65] PGE_2 also can show its growth-promoting effects through the induction of HER2/Neu expression,[66] which we found to be up-regulated in COX-2 transgenic pancreas, again recapitulating the human counterparts.[53] Additional effects of aberrant COX-2 expression/activity were the increased steady-state levels of Ras protein and GTP-bound Ras, indicating an activation of Ras. Recently, PGE_2 was found to stimulate the activation of the Ras-mitogen–activated protein kinase cascade in the human colon carcinoma cell line HCA-7, an effect that led to Ras-dependent stimulation of growth.[67] Hence, a PGE_2-Ras–dependent stimulation of growth also may contribute to the hyperproliferation of duct cells in K5 COX-2 transgenic pancreas.

The spatial extension of these lesions may be assumed to indirectly initiate acinar tissue damage by compression, finally resulting in a disappearance of cells within this compartment and a subsequent inflammatory and fibrotic reaction. Although the mechanisms of initial tissue damage may be different, there are, at least at the histologic level, similar patterns of fibroinflammatory

reaction in human adenocarcinomas and also in obstructive chronic pancreatitis.[68] Likewise, abundant macrophages, CD4-positive T cells, and CD45/B220-positive B cells were present in the COX-2 transgenic pancreas. Despite the presence of this cellular infiltrate, the high tissue level of PGE_2 may impair an immune reaction against atypical cells because PGE_2 has been described as a complex immunomodulator that influences macrophages, T cells, and B cells, with the overall result of an enhanced T-helper 2 and inhibited T-helper 1 response.[69] A determination of the cytokine profile and levels in COX-2 transgenic pancreas will help to elucidate the mechanisms underlying the observed inflammatory reaction.

The observation that the PDX-1–promoter–driven expression of the K-rasG12D mutant correlates with aberrant COX-2 expression in PanINs of these mice[57] suggests that COX-2 is a downstream target of mutated K-ras. In the COX-2 transgenic pancreas, however, a progression of PanIN to PDAC was not observed, although Ras activation was measured. On the other hand the mutational Ras activation in PDX-1/K-rasG12D mice developed PDAC with a low frequency. An earlier appearance of PanIN lesions and an increased progression rate to PDAC was achieved only by the additional deficiency of Ink4/Arf in the pancreas of the PDX-1/K-rasG12D mice.[70] According to a recent study, the con-

comitant endogenous expression of the mutant Trp53R172H and K-rasG12D in mouse pancreas also accelerated the development of invasive and widely metastatic PDAC that resembled the cognate human cancer.[71] The K5 COX-2 transgenic mouse model offers an unique possibility of identifying the different molecular pathways involved in the formation of SCA-, IPMN-, and PanIN-like lesions and their malignant progression.

In summary, strong evidence is presented for the causal relationship between COX-2–mediated PG synthesis and the described phenotype, substantiated by the fact that the inhibition of the COX-2 activity by the application of the COX-2–selective inhibitor Celebrex suppressed the development of the phenotype. These data provide a strong mechanistic basis for clinical studies with COX-2–selective inhibitors as adjuvants to chemotherapy and/or radiotherapy of patients with pancreatic cancer.

References

1. Adsay NV, Klimstra DS. Cystic forms of typically solid pancreatic tumors. Semin Diagn Pathol 2000;17:81–88.
2. Brugge WR, Lauwers GY, Sahani D, Fernandez-del Castillo C, Warshaw AL. Cystic neoplasms of the pancreas. N Engl J Med 2004;351:1218–1226.
3. Kosmahl M, Pauser U, Peters K, Sipos B, Lüttges J, Kremer B, Klöppel G. Cystic neoplasms of the pancreas and tumor-like lesions with cystic features: a review of 418 cases and a classification proposal. Virchows Arch 2004;445:168–178.
4. Kosmahl M, Wagner J, Peters K, Sipos B, Kloppel G. Serous cystic neoplasms of the pancreas: an immunohistochemical analysis revealing alpha-inhibin neuron-specific enolase and MUC 6 as new markers. Am J Surg Pathol 2004;28:339–346.
5. Compagno J, Oertel JE. Microcystic adenomas of the pancreas (glycogen-rich cystadenomas): a clinicopathologic study of 34 cases. Am J Clin Pathol 1978;69:289–298.
6. Alpert LC, Truong LD, Bossart MI, Spjut HJ. Microcystic adenoma (serous cystadenoma) of the pancreas. A study of 14 cases with immunohistochemical and electron-microscopic correlation. Am J Surg Pathol 1988;12:251–263.
7. Compton CC. Serous cystic tumors of the pancreas. Semin Diagn Pathol 2000;17:43–55.
8. Gerdes B, Wild A, Wittenberg J, Barth P, Ramaswamy A, Kersting M, Luttges J, Kloppel G, Bartsch DK. Tumor-suppressing pathways in cystic pancreatic tumors. Pancreas 2003;26:42–48.
9. Hruban RH, Takaori K, Klimstra SS, Adsay V, Albores-Saavedrs J, Biankin AV, Biankin SA, Compton C, Fukushima N, Goggins M, Kato Y, Kloppel G, Longnecker DS, Luttges J, Maitra A, Offerhaus GJ, Shimizu M, Yonezawa S. An illustrated consensus on the classification of pancreatic intraepithelial neoplasia and intraductal papillary mucinous neoplasms. Am J Surg Pathol 2004;28:977–987.
10. Z'graggen K, Rivera JA, Compton CC, Pins M, Werner J, Fernandez-del Castillo C, Rattner DW, Lewandrowski KB, Rustgi AK, Warshaw AL. Prevalence of activating K-ras mutations in the evolutionary stages of neoplasia in intraductal papillary mucinous tumors of the pancreas. Ann Surg 1997;226:491–498.
11. Iacobuzio-Donahue CA, Wilentz RE, Argani P, Yeo CJ, Cameron JL, Kern SE, Hruban RH. Dpc4 protein in mucinous cystic neoplasms of the pancreas: frequent loss of expression in invasive carcinomas suggests a role in genetic progression. Am J Surg Pathol 2000;24:1544–1548.
12. Wada K. P16 and p53 gene alterations and accumulations in the malignant evolution of intraductal papillary-mucinous tumors of the pancreas. J Hepatobiliary Pancreat Surg 2002;9:76–85.
13. Sasaki S, Yamamoto H, Kaneto H, Ozeki I, Adachi Y, Takagi H, Matsumoto T, Itoh H, Nagakawa T, Miyakawa H, Muraoka S, Fujinaga A, Suga T, Satoh M, Itoh F, Endo T, Imai K. Differential roles of alterations of p53 p16 and SMAD4 expression in the progression of intraductal papillary-mucinous tumors of the pancreas. Oncol Rep 2003;10:21–25.
14. Bardeesy N, DePinho RA. Pancreatic cancer biology and genetics. Nature Rev 2002;2:897–902.
15. Hruban RH, Goggins M, Parsons J, Kern SE. Progression model for pancreatic cancer. Clin Cancer Res 2000;6:2969–2972.
16. Yip-Schneider MT, Barnard DS, Billings SD, Cheng L, Heilman DK, Lin A, Marshall SJ, Crowell PL, Marshall MS, Sweeney CJ. Cyclooxygenase-2 expression in human pancreatic adenocarcinomas. Carcinogenesis 2000;21:139–146.
17. Maitra A, Ashfaq R, Gunn CR, Rahman A, Yeo CJ, Sohn TA, Cameron JL, Hruban RH, Wilentz RE. Cyclooxygenase 2 expression in pancreatic adenocarcinoma and pancreatic intraepithelial neoplasia: an immunohistochemical analysis with automated cellular imaging. Am J Clin Pathol 2002;118:194–201.
18. Niijima M, Yamaguchi T, Ishihara T, Hara T, Kato K, Kondo F, Saisho H. Immunohistochemical analysis and in situ hybridization of cyclooxygenase-2 expression in intraductal papillary-mucinous tumors of the pancreas. Cancer 2002;94:1565–1573.
19. Iacobuzio-Donahue CA, Ashfaq R, Maitra A, Adsay NV, Shen-Ong GL, Berg K, Hollingsworth MA, Cameron JL, Yeo CJ, Kern SE, Goggins M, Hruban RH. Highly expressed genes in pancreatic ductal adenocarcinomas: a comprehensive characterization and comparison of the transcription profiles obtained from three major technologies. Cancer Res 2003;63:8614–8622.
20. Friess H, Ding J, Kleeff J, Fenkell L, Rosinski JA, Guweidhi A, Reidhaar-Olson JF, Korc M, Hammer J, Buchler MW. Microarray-based identification of differentially expressed growth- and metastasis-associated genes in pancreatic cancer. Cell Mol Life Sci 2003;60:1180–1199.
21. Sato N, Fukushima N, Maitra A, Iacobuzio-Donahue CA, Tarda van Heek N, Cameron JL, Yeo CJ, Hruban RH, Goggins M. Gene expression profiling identifies genes associated with invasive intraductal papillary mucinous neoplasms of the pancreas. Am J Pathol 2004;164:903–914.
22. Prasad NB, Biankin AV, Fukushima N, Aitra A, Dhara S, Elkahloun AG, Hruban RH, Goggins M, Leach SD. Gene expression profiles in pancreatic intraepithelial neoplasia reflect the effects of hedgehog signaling on pancreatic ductal epithelial cells. Cancer Res 2005;65:1619–1626.
23. Simmons DL, Botting RM, Hla T. Cyclooxygenase isozymes: the biology of prostaglandin synthesis and inhibition. Pharmacol Rev 2004;56:387–433.
24. Helliwell RJA, Adams LF, Mitchell MD. Prostaglandin synthases: recent developments and a novel hypothesis. Prostaglandins Leukot Essent Fatty Acids 2004;70:101–113.
25. Hata AN, Breyer RM. Pharmacology and signaling of prostaglandin receptors: multiple roles in inflammation and immune modulation. Pharmacol Ther 2004;103:147–166.
26. Thun MJ, Henley SJ, Patrono C. Nonsteroidal anti-inflammatory drugs as anticancer agents: mechanistic pharmacologic and clinical issues. J Natl Cancer Inst 2002;94:252–266.
27. Oshima M, Dinchuk JE, Kargman SL, Oshima H, Hancock B, Kwong E, Trazaskos JM, Evans JF, Taketo MM. Suppression of intestinal polyposis in APC716 knockout mice by inhibition of cyclooxygenase-2 (COX-2). Cell 1996;87:803–809.
28. Chulada PC, Thompson MB, Mahler JF, Doyle CM, Gaul BW, Lee C, Tiano HF, Morham SG, Smithies O, Langenbach R.

Genetic disruption of Ptgs-1 as well as of Ptgs-2 reduces intestinal tumorigenesis in min mice. Cancer Res 2000;60:4705–4708.

29. Neufang G, Fürstenberger G, Heidt M, Marks F, Müller-Decker K. Abnormal differentiation of epidermis in transgenic mice constitutively expressing cyclooxygenase-2 in skin. Proc Natl Acad Sci U S A 2001;98:7629–7634.

30. Liu CH, Chang SH, Narko K, Trifan OC, Wu MT, Smith E, Haudenschild C, Lane TF, Hla T. Overexpression of cyclooxygenase-2 is sufficient to induce tumorigenesis in transgenic mice. J Biol Chem 2001;276:18563–18569.

31. Müller-Decker K, Neufang G, Berger I, Neumann M, Marks F, Fürstenberger G. Transgenic cyclooxygenase-2 overexpression sensitizes mouse skin for carcinogenesis. Proc Natl Acad Sci U S A 2002;99:12483–12488.

32. Tiano HF, Loftin CD, Akunda J, Lee CA, Spalding J, Sessoms A, Dunson DB, Rogan EG, Morham SG, Smart RC, Langenbach R. Deficiency of either cyclooxygenase (COX)-1 or COX-2 alters epidermal differentiation and reduces mouse skin tumorigenesis. Cancer Res 2002;62:3395–3401.

33. Fischer SM, Conti CJ, Viner J, Aldaz CM, Lubert RA. Celecoxib and difluoromethylornithine in combination have strong therapeutic activity against UV-induced skin tumors in mice. Carcinogenesis 2003;49:709–713.

34. Subbaramaiah K, Dannenberg AJ. Cyclooxygenase 2: a molecular target for cancer prevention and treatment. Trends Pharmacol Sci 2003;24:96–102.

35. Steinbach G, Lynch PM, Phillips RKS, Wallace MH, Hawk E, Gordon GB, Wakabayashi N, Saunders B, Shen Y, Fujimura T, et al. The effect of celecoxib, a cyclooxygenase-2 inhibitor, in familial adenomatous polyposis. N Engl J Med 2000;342:1946–1952.

36. Gasparini G, Longo R, Sarmiento R, Morabito A. Inhibitors of cyclo-oxygenase 2: a new class of anticancer agents? Lancet Oncol 2003;4:605–615.

37. Dannenberg AJ, Lippmann SM, Mann JR, Subbaramaiah K, DuBois RN. Cyclooxygenase-2 and epidermal growth factor receptor: pharmacologic targets for chemoprevention. J Clin Oncol 2005;23:254–266.

38. Molina MA, Sitja-Arnau M, Le Moine MG, Frazier ML, Sinicrope FA. Increased cyclooxygenase-2 expression in human pancreatic carcinomas and cell lines: growth inhibition by nonsteroidal anti-inflammatory drugs. Cancer Res 1999;59:4356–4362.

39. Okami J, Yamamoto H, Fujiwara Y, Tsujie M, Nagano H, Dono K, Umeshita K, Ishikawa O, Sakon M, et al. Overexpression of cyclooxygenase-2 in carcinoma of the pancreas. Clin Cancer Res 1999;5:2018–2024.

40. Tucker ON, Dannenberg AJ, Yang EK, Zhang FY, Teng L, Daly JM, Soslow RA, Masferrer JL, Woerner BM, Koki AT, Fahey TJ 3rd. Cyclooxygenase-2 expression is up-regulated in human pancreatic cancer. Cancer Res 1999;59:987–990.

41. Merati K, Said Siadaty M, Andrea A, Sarkar F, Ben-Josef E, Mohammed R, Philip P, Shields AF, Vaitkevicius V, Grignon DJ, Adsay NV. Expression of inflammatory modulator COX-2 in pancreatic ductal adenocarcinoma and its relationship to pathologic and clinical parameters. Am J Clin Oncol 2001;24:447–452.

42. Kokawa A, Kondo H, Gotoda T, Ono H, Saito D, Nakadaira S, Kosuge T, Yoshida S. Increased expression of cyclooxygenase-2 in human pancreatic neoplasms and potential for chemoprevention by cyclooxygenase inhibitors. Cancer 2001;15:333–338.

43. O'Neill GP, Ford-Hutchinson AW. Expression of mRNA for cyclo-oxygenase-1 and cyclooxygenase-2 in human tissues. FEBS Lett 1993;330:156–160.

44. Franco L, Doria D, Bertazzoni E, Benini A, Bassi C. Increased expression of inducible nitric oxide synthase and cyclooxygenase-2 in pancreatic cancer. Prostaglandins Other Lipid Mediat 2004;73:51–58.

45. Nishikawa A, Furukawa F, Lee IS, Tanaka T, Hirose M. Potent chemopreventive agents against pancreatic cancer. Curr Cancer Drug Targets 2004;4:363–373.

46. Takahashi M, Furukawa F, Toyoda K, Sato H, Hasegawa R, Imaida K, Hayashi Y. Effects of various prostaglandin synthesis inhibitors on pancreatic carcinogenesis in hamsters after initiation with N-nitrosobis(2-oxopropyl)amine. Carcinogenesis 1990;11:393–395.

47. Raut CP, Nawrocki S, Lashinger LM, Davis DW, Khanbolooki S, Xiong H, Ellis LM, McConkey DL. Celecoxib inhibits angiogenesis by inducing endothelial cell apoptosis in human pancreatic tumor xenografts. Cancer Biol Ther 2004;3:1217–1224.

48. Müller-Decker K, Berger I, Ackermann K, Ehemann V, Zoubova S, Aulmann S, Pyerin W, Fürstenberger G. Cystic duct dilatations and proliferative epithelial lesions in mouse mammary glands upon keratin 5 promoter-driven overexpression of cyclooxygenase-2. Am J Pathol 2005;166:575–584.

49. Moll R, Dhouailly D, Sun TT. Expression of keratin 5 as a distinctive feature of epithelial and biphasic mesotheliomas. Virchows Arch 1989;58:129–145.

50. Real FX, Vila MR, Skoudy A, Ramaekers FC, Corominas JM. Intermediate filaments as differentiation markers of exocrine pancreas. II Expression of cytokeratins of complex and stratified epithelia in normal pancreas and in pancreas cancer. Int J Cancer 1993;54:720–727.

51. Talley JJ, Brown DL, Carter JS, Graneto MJ, Koboldt CM, Masferrer JL, Perkins WE, Rogers RS, Shaffer AF, Zhang YY, Seibert K. 4-[5-Methyl-3-phenylisoxazol-4-yl]- benzenesulfonamide valdecoxib: a potent and selective inhibitor of COX-2. J Med Chem 2000;43:775–777.

52. Grapin-Botton A. Ductal cells of the pancreas. Int J Biochem Cell Biol 2005;7:504–510.

53. Day JD, Digiueseppe JA, Yeo C, Lai-Goldmann M, Anderson SM, Goodman SN, Kern SE, Hruban RH. Immunohistochemical evaluation of HER2/neu expression in pancreatic adenocarcinoma and pancreatic intraepithelial neoplasms. Hum Pathol 1996;27:119–124.

54. Klein RD, Van Pelt CS, Sabichi AL, Dela Cerda J, Fischer SM, Furstenberger G, Muller-Decker K. Transitional cell hyperplasia and carcinomas in urinary bladders of transgenic mice with keratin 5 promoter-driven cyclooxygenase-2 overexpression. Cancer Res 2005;65:1808–1813.

55. Bardeesy N, Morgan J, Sinha M, Signorotti S, Srivastava S, Loda M, Merlino G, DePinho RA. Obligate roles for p16(Ink4a) and p19(Arf)-p53 in the suppression of murine pancreatic neoplasia. Mol Cell Biol 2002;22:635–643.

56. Brembeck FH, Schreiber FS, Deramaudt TB, Craig L, Rhoades B, Swain G, Grippo P, Stoffers DA, Silberg DG, Rustgi AK. The mutant K-ras oncogene causes pancreatic periductal lymphocytic infiltration and gastric mucous neck cell hyperplasia in transgenic mice. Cancer Res 2003;63:2005–2009.

57. Hingorani SR, Petricoin EF, Maitra A, Rajapakse V, King C, Jacobetz MA, Ross S, Conrads TP, Veenstra TD, Hitt BA, Kawaguchi Y, Johann D, Liotta LA, Crawford HC, Putt ME, Jacks T, Wright CV, Hruban RH, Lowy AM, Tuveson DA. Pre-invasive and invasive ductal pancreatic cancer and its early detection in the mouse. Cancer Cell 2003;4:437–450.

58. Leach SD. Mouse models of pancreatic cancer: the fur is finally flying. Cancer Cell 2004;5:7–11.

59. Grippo PJ, Nowlin PS, Demeure MJ, Longnecker DS, Sandgren EP. Pre-invasive pancreatic neoplasia of ductal phenotype induced by acinar cell targeting of mutant Kras in transgenic mice. Cancer Res 2003;63:2016–2019.

60. Thayer SP, Di Magliano MP, Helser PW, Nielsen CM, Roberts DJ, Lauwers GY, Qi YP, Gysin S, Del Castillo CF, Yajnik V, Antonin B,

McMahon M, Warshaw AL, Hebrok M. Hedgehog is an early and late mediator of pancreatic cancer tumorigenesis. Nature 2003;425:851–856.

61. Edlund H. Pancreatic organogenesis-developmental mechanisms and implications for therapy. Nature 2002;3:524–532.

62. Schneider G, Siveke JT, Eckel F, Schmid RM. Pancreatic cancer: basic and clinical aspects. Gastroenterology 2005;128:1606–1625.

63. Takaori K, Kobashi Y, Matsusue S, Matsui K, Yamamoto T. Clinicopathological features of pancreatic intraepithelial neoplasias and their relationship to intraductal papillary-mucinous tumors. J Hepatobiliary Pancreat Surg 2003;10:125–136.

64. Pai R, Soreghan B, Szabo IL, Pavelka M, Baatar D, Tarnawski AS. Prostaglandin E2 transactivates EGF receptor: a novel mechanism for promoting colon cancer growth and gastrointestinal hypertrophy. Nat Med 2002;8:289–293.

65. Shao J, Lee SB, Guo H, Evers BM, Sheng H. Prostaglandin E2 stimulates growth of colon cancer cells via induction of amphiregulin. Cancer Res 2003;63:5218–5223.

66. Benoit V, Relic B, Leval XX, Chariot A, Merville MP, Bours V. Regulation of HER-2 oncogene expression by cyclooxygenase-2 and prostaglandin E2. Oncogene 2004;23:1631–1635.

67. Wang D, Buchanan FG, Wang H, Dey SK, DuBois RN. Prostaglandin E2 enhances intestinal adenoma growth via activation of the ras-mitogen-activated protein kinase cascade. Cancer Res 2005;65:1822–1829.

68. Klöppel G. Fibrosis of the pancreas: the initial tissue damage and the resulting pattern. Virchows Arch 2004;445:1–8.

69. Harris SG, Padilla J, Koumas L, Ray D, Phipps RP. Prostaglandins as modulators of immunity. Trends Immunol 2002;23:144–150.

70. Aguirre AJ, Bardeesy N, Sinha M, Lopez L, Tuveson DA, Horner J, Redston MS, DePinho RA. Activated Kras and Ink4a/Arf deficiency cooperate to produce metastatic pancreatic ductal adenocarcinoma. Genes Dev 2003;17:3112–3126.

71. Hingorani SR, Wang L, Multani AS, Combs C, Deramaudt TB, Hruban RH, Rustgi AK, Chang S, Tuveson DA. Trp53R172H and KrasG12D cooperate to promote chromosomal instability and widely metastatic pancreatic ductal adenocarcinoma in mice. Cancer Cell 2005;7:469–483.